EFFECT OF HEAT TREATMENT AND TEST METHOD ON DBTT OF A V-5Cr-5Ti ALLOY - Huaxin Li (Associated Western Universities--Northwest Division), M. L. Hamilton and R. H. Jones (Pacific Northwest Laboratory)*

OBJECTIVE

The purpose of this research is to investigate further the effect of heat treatment (HT) on fracture properties of a V-5Cr-5Ti alloy in the temperature range -190 to 90°C, and also to investigate how its DBTT depends on HT and test method.

SUMMARY

Specimens annealed at 1125°C for 1 h and furnace cooled were brittle at room temperature (RT) and experienced a mixture of intergranular and cleavage fracture. Fracture toughness (JIQ) at RT was 52 kJ/m^2 and the Charpy-V impact fracture energy (IFE) on one-third scaled specimens was 0.2 J. While material exhibited high fracture toughness at 100°C (J_{IQ} was 485 kJ/m^2) and did not fracture during an impact test, the fracture surface contained a mixture of dimple and intergranular fracture, with intergranular fracture making up 40% of the total fracture surface. The ductile to brittle transition temperature (DBTT) was estimated to be above RT from the IFE vs. temperature curve. When material was given an additional annealing at 890°C for 24 h, it became ductile at RT and fractured by microvoid coalescence. The J_{IQ} value increased from 52 kJ/m^2 to ≈1100 kJ/m^2. During impact tests, the specimens did not fracture at -100°C and warmer due to a large amount of plastic deformation. The DBTT was -100°C. However, when evaluated by J-integral testing, the material became brittle at -50°C and fractured by cleavage, yielding a J_{IQ} value of 50 kJ/m^2. The DBTT$_J$ estimated from J_{IQ} vs. temperature curve was above -50°C, 50°C higher than that from the IFE vs. temperature curve. The result indicated that the V-5Cr-5Ti alloy was sensitive to crack acuity. Auger electron microscopy analysis showed significant sulfur enrichment (6 at%) on grain boundaries in the specimens annealed only at 1125°C, but only 0.9 at% on grain boundaries if the additional annealing at 890°C was given. Moreover, more second phase particles were found in the specimens annealed at 1125°C plus 890°C. Energy dispersive x-ray spectroscopy analysis of the particles indicated that they contained higher Ti concentration. The results indicated that the improved toughness of the specimens annealed at 1125°C plus 890°C probably resulted from the reduced S concentration on the grain boundaries and precipitation of the second phases. It was found that the embrittlement was thermodynamically reversible because the embrittlement could be restored by giving the ductile material additional annealing at 1125°C for 1h.

PROGRESS AND STATUS

Introduction

A vanadium (V)-based alloy with 5%(wt) Cr and 5%(wt) Ti (V-5Cr-5Ti) is being considered as a candidate structural material for a fusion energy system. Besides retaining good strength and ductility at both ambient and elevated temperatures, V-based alloys possess some unique neutronic properties as

---

*Pacific Northwest Laboratory is operated for the U.S. Department of Energy by Battelle Memorial Institute under Contract DE-AC06-76RLO 1830.

austenitic and Ferritic steels. Low neutron activation in the short-term, and especially in intermediate and long terms, and low biological hazard potential are particularly attractive properties of vanadium alloys. However, the alloy was found to be brittle at room temperature (RT) and experienced mixed intergranular and cleavage fracture when annealed at 1125°C for 1 h and then furnace cooled (HT1)[1]. While it became ductile at 100°C, it still failed by intergranular and microvoid coalescence modes[2,3]. However, if an additional heat treatment of 890°C for 24 h (HT2) was given, the material become ductile[4,5] Auger electron spectroscopy analysis showed a significant enrichment of sulfur (S) on grain boundaries (6% at) in a specimen annealed at 1125°C for 1 h[4,5], as compared with that HT2 specimens (0.9 %at). Besides, optical microscopic investigation found significantly more second phase in HT2 specimens. In this study, the reversibility of the embrittlement investigated and the DBTTs were evaluated by Charpy-V impact and fracture toughness (J-integral) testing.

Material and Experimental Methods

A 6.35-mm-thick V-5Cr-5Ti alloy plate (ANL #BL-63) was produced by Teledyne Wah Chang, Albany, OR. The chemical composition of the plate (as provided by the vendor) is listed in Table 1.

Table 1. Chemical Composition of V-5Cr-5Ti

(in wt%)	Cr	Ti	(in wt ppm)	O	C	N	Si	V
	4.6	5.1		440	73	28	310	bal.

The following heat treatments were investigated for grain boundary chemistry.
1. Heat treatment 1 (HT1): 1125°C/1 h/furnace cooled
2. Heat treatment 2 (HT2): HT1 plus 890°C/24 h/furnace cooled
3. Heat treatment 3 (HT3): HT1 plus HT2 plus 1125°C/1 h/furnace cooled

All heat treatments were conducted in a vacuum of 1.33×10^{-5} Pa. Grain boundary chemistry was analyzed by means of a scanning Auger electron spectrometer (AES) (PERKIN-ELMER-660). Specimens were cooled by extracting heat with liquid nitrogen, and were fractured in the AES chamber in a vacuum of 1×10^{-7} Pa or better. Auger spectra were taken at an accelerating voltage of 5 kV and an incident electron current of about 250 nA. At least 22 intergranular facets and 6 grain interiors were analyzed; sometimes duplicate samples were tested. Microstructure was analyzed using an optical microscope and a scanning electron microscope (SEM). Specimens were etched for the same length of time using a solution composed of 30 ml lactic, 10 ml HNO_3, and 10 ml HF Fracture surfaces were also investigated using SEM. Energy dispersive x-ray spectroscopy (EDS) was used to determine semiquantitatively the composition of second particles in HT2 specimens.

The specimens used for fracture toughness and Charpy-V impact tests were cut in the T-L orientation as specified in ASTM E399-90. The compact tension specimen was 25.4 mm wide and 6.35 mm thick. ASTM E813-89 was used to determine critical J-integrals (J_{IQ}), and ASTM E399-90 was used to determine the critical stress intensity factor (K_{IQ}). The subscript "Q" is used because our specimen size did not satisfy plane strain conditions. Mechanical properties, listed in Table 2, from another heat of V-5Cr-5Ti were used for determination of J_{IQ} values. Charpy-V impact specimens of 23.6 x 3.33 x 3.33 mm (one-third scaled) were tested on the HT2 specimens in the range -190°C to RT, and on the HT1 and HT3 specimens at RT and 90°C to estimate the DBTTs. Fracture toughness was determined at RT and 100°C on the HT1

specimen, and -50°C and RT on the HT2 specimens.

Table 2. Mechanical Properties of a V-5Cr-5Ti Alloy

Temp. (°C)	Yield strength (MPa)	UTS* (MPa)	Elongation (%)
25	387	454	34
100	325	420	33

* UTS: ultimate tensile strength.

Fracture toughness was determined by the J-integral test method for an HT1 specimen tested at 100°C and an HT2 specimen tested at RT. For an HT1 specimen tested at RT and an HT2 specimen tested at -50°C, fracture toughness was measured using the K-test method. The K_{IQ} values were then converted to J_{IQ} values by means of Eq. 1. Temperatures were controlled within ±5°C during testing using either a heating tape or a refrigerator, respectively. The single-specimen technique was used in this study, which allows a J-R curve (J-integral vs. crack extension, Δa) to be generated with one specimen. At least 40 pairs of J-Δa data were used to construct a J-R curve.

$$J\!\mid\!S\!\mid\!DO8(IQ) = \!\mid\!F\ (K\!\mid\!S(2,IQ)\!\mid\!D\!\mid\!FO4()(1\!\mid\!D\!\mid\!FO4()-\!\mid\!D\!\mid\!FO4()n\!\mid\!S(\ ,2)),E) \quad (1)$$

Where E is Young's modulus and n is a Poisson ratio.

Results

Effect of Heat Treatment on Grain Boundary S Concentration and Microstructure

a. On Grain Boundary Chemistry

The specimens subjected to HT1 were brittle at RT and fractured with a mixture of intergranular and cleavage modes, indicating that the grain boundary strength was low. AES analysis of two specimens showed significant enrichment of S (6 at%) in more than 40 intergranular facets, as compared to 0.3 at% on the cleavage facets. In order to obtain intergranular facets, HT2 specimens had to be charged with hydrogen before being fractured in the AES chamber. The effect of heat treatment on grain size, grain boundary chemistry, and microstructure is summarized in Table 3. Phosphorus, oxygen, nitrogen, and carbon concentrations were also investigated using AES, but their concentrations did not vary significantly with heat treatments, so only S was listed in Table 3. From Table 3, it is evident that HT2 gives much lower grain boundary S concentration than HT1 does.

Table 3. Effect of Heat Treatment on Grain Boundary S Concentrations and Number Precipitates

Heat treatments	Grain Size (μm)	Grain Boundary S (at%)	Number of Precipitates
1125°C/1 h	45	6.0	few
1125°C/890°C/24 h	45	0.9	many
As received	37	NM	some

NM: not measured

b. On Microstructure

The HT2 also produced significantly more second-phase precipitates than HT1, as shown in Figs. 1a and 1b. SEM photos at higher magnification showed that the HT2 specimen contained pores and second phase particles, as shown in Figs. 2 and 3. EDS analysis showed that the second phase was enriched slightly with Ti, as compared with that of the matrix. The chemical composition from the second phase and the matrix is given in Table 4. It should be noticed that due to the small size of particles and the penetration of SEM electron beam, the composition for the second phase must be a mixture of the second phase and matrix. The actual Ti concentration in the second phase will be higher than that in Table 4. The pores probably resulted from local dissolution during etching. This feature suggested that HT2 may produce two types of precipitates because the HT1 specimen did have as many pores when etched identically. In order to gain more accurate chemical composition and nature of the dissolved particles, TEM examination is under way.

Table 4. Chemical Composition (%wt) of the Second Phase in HT2 Specimen (by EDS)

Location	V	Ti	Cr
Matrix	88.1	7.0	4.9
Second Phase	87.2	8.0	4.8

Mechanical Properties

a. Specimens Subjected to HT1

The dependence of IFE on temperature is presented in Fig. 4. The specimens treated using HT1 were brittle at RT and below. The IFE at RT was 0.2 J. At 90°C the specimen did not fracture due to a large amount of plastic deformation at the notch tip. The data in Fig. 4 present only the nominal energy consumed

amount of plastic deformation at the notch tip. The data in Fig. 4 present only the nominal energy consumed deforming the specimens during testing. The energy does not include the portion for crack initiation and propagation; therefore, the IFE could not be determined. However, based on an upper shelf IFE (about 12 J) obtained from another test[5], the IEF for the sample could be as high as 12 J. An upward arrow is superimposed on some of the data in Fig. 4 to indicate that the IFE should be higher. The DBTT is apparently greater than RT.

Fig. 5 shows the dependence of fracture toughness on testing temperature. J_{IQ} at RT was 52 kJ/m^2. The specimen fractured with a mixture of intergranular and cleavage failure, as shown in Fig. 6. Fig. 6b shows that cleavage facets appear to initiate at the grain boundaries and propagate through the grains. When tested at 100°C, the material was ductile and exhibited stable crack growth. J_{IQ} was about 485 kJ/m^2 and the tearing modulus was 250 mJ/m^3. Despite the high J_{IQ} value at 100°C, the fracture surface consisted of intergranular and microvoid coalescence features[2]. The intergranular portion made up about 40% of the total fracture surface. However, the grains experienced a large amount of plastic deformation before they fractured along the grain boundaries, yielding high fracture toughness.

b. Specimens Subjected to HT2

The HT2 specimens were very ductile at RT. As a result, a complete J-R curve could not be constructed with the compact tension specimen. The J_{IQ} estimated from the partial J-R curve (Fig. 7) is about 1100 kJ/m^2. The specimen fractured by microvoid coalescence, as shown in Fig. 8a. The fracture toughness was sensitive to temperature: J_{IQ} at -50°C was 45 kJ/m^2, only about one-twentieth that at RT. The fracture mode also changed to cleavage fracture, as shown in Fig. 8b. The dependence of fracture toughness on testing temperature is shown in Fig. 5.

Charpy testing failed to cause fracture at temperatures of -100°C and higher (Fig. 4) due to a large amount of plastic deformation; therefore, IFEs could not be determined. The dashed line in Fig. 3 represents the estimated dependence of IFE of HT2 specimens on testing temperature. Based on the data from Ref. 5, 12 J IFE was chosen as the upper shelf IFE (Fig. 4). The IFEs were 4 J at -115°C and 0.2 J at -190°C. The DBTT was estimated to be -110°C.

Table 5. Effect of Heat Treatment and Temperature on Fracture Toughness

Heat treatment	J_{IQ} (kJ/m^2) at -50°C	at RT	at 100°C	Fracture at RT
HT1	NM	52	485	IG* & Cleavage
HT2	45	1100	NM	Dimpled

* IG: intergranular; NM: not measured.

c. Specimens Subjected to HT3

The dependence of IFE on test temperature for the HT3 specimens is shown in Fig. 4 The HT3 specimens were brittle at RT. The IFE at RT was only 3 J and fell in the lower shelf energy range although it was higher than that of the HT1 specimen. SEM showed that the specimen fractured by a mixture of intergranular and cleavage modes, as shown in Fig 8. At 90°C, the specimen did not fracture due to a large amount of plastic deformation at the notch tip. An upward arrow is superimposed to indicate that the IFE should be higher. The DBTT is apparently greater than RT. This result indicated that the embrittlement was reversible, though not completely. The effects of heat treatment and temperature on fracture properties of the V-5Cr-5Ti alloy are summarized in Figs. 3 and 4, and also in Tables 5 and 6

Table 6. Effect of Heat Treatment and Test Method on DBTT

Heat treatment	DBTT (°C)	$DBTT_J$ (°C)
HT1	>RT	>RT
HT2	≈ -100	≈-30
HT3	>RT	NM

NM: not measured.

Discussion

The mixture of intergranular and cleavage fracture modes in the HT1 specimens appears to result from a low grain boundary fracture strength. It is known that impurity segregation to grain boundaries in a metallic material can reduce grain boundary strength, and that interstitial impurities can enhance cleavage fracture. Optical microscopy and SEM analysis of HT1 and HT2 specimens showed that second-phase formation occurred at about 890°C in this V-5Ti-5Cr alloy. Because the grain size in both HT1 and HT2 specimens was almost identical, the increase in fracture toughness of the HT2 specimens probably resulted from two factors: 1) HT2 increases grain boundary strength by reducing grain boundary S concentration, and 2) HT2 improves the ductility of grains by decreasing interstitial impurity concentration via precipitate formation. The reversibility of the brittleness suggested that dissolution of the second phases occurred at 1125°C, which caused the brittleness in the V-5Ti-5Cr alloy. TEM analysis of the precipitates is underway.

Conclusion

1. Specimens of V-5Cr-5Ti annealed at 1125°C/1 h (HT1) were brittle at RT and fractured by intergranular and cleavage modes. The J_{IQ} was about 52 kJ/m^2. At 100°C, specimens were ductile, giving a J_{IQ} value of 485 kJ/m^2, but fracture surfaces were composed of both intergranular and dimple fracture. The DBTT as determined from impact tests was higher than RT.
2. Annealing specimens at 1125°C/1 h and then at 890°C/24 h (HT2) improved the RT fracture toughness dramatically, from 52 to about 1100 kJ/m^2, and changed the mode of fracture to microvoid coalescence. Specimens were brittle at -50°C, yielding a J_{IQ} value of 45 kJ/m^2. The DBTT was -100°C.
3. The HT2 reduced grain boundary S concentration (0.9 at%) greatly as compared to HT1 (6 at%) and produced more precipitates.

Acknowledgments

We are grateful to Dr. M. L. Grossbeck of Oak Ridge National Lab. for supplying us with the V-5Cr-5Ti alloy. The assistance of Mr. J. L. Humason at Pacific Northwest Laboratory in developing the test methods is gratefully acknowledged. This research was supported by the Office of Fusion Energy of the U. S. Department of Energy under Contract DE-AC06-76RLO 1830 with Battelle Memorial Institute.

References

1. Huaxin Li, R. H. Jones, and J. P. Hirth, Fusion Reactor Materials Semiannual Progress Report. DOE/ER-0313/16, Oak Ridge National Lab., Oak Ridge, TN (March 1994), pp. 279-92.
2. Huaxin Li, R. H. Jones, and J. P. Hirth, Scripta Metall. Mater., 32 (1995), pp. 611-16.
3. R. H. Jones, in Mechanical Properties and Phase Transformations in Engineering Materials, S. D. Antolovich, R. O. Ritchie, and W. W. Gerberich, eds. The Metallurgical Society of AIME, 1986, pp. 227-49.
4. B. A. Loomis, J. Gazda, L. J. Nowicki, and D. L. Smith, "Relationship of Microstructure and Mechanical Properties of V-Cr-Ti Alloys," CFRM-6/Ref. No. H016, Sixth International Conference

5. Huaxin Li, M. L. Hamilton, and R. H. Jones, Fusion Reactor Materials Semiannual Progress Report. DOE/ER-0313/17, Oak Ridge National Lab., Oak Ridge, TN (October 1994), in press.

Fig. Captions

Fig. 1. The dependence of critical total J-integrals of V-5Cr-5Ti on crack inclination angles and temperatures. The results for a reduced activation Ferritic/martensitic steel (F-82H) is included for comparison.

Fig. 2. The geometry of the compact tension specimen used in this study.

Fig. 3. Optical micrographs (50 X) showing microstructures resulting from: a.) as-received; b.) 1050°C/ 1h/ furnace cooled (FC); c.) 1125°C/ 1h/ FC; and d.) 1125°C/ 1h/ FC plus 890°C/ 24h/ FC.

Fig. 4. Fracture surfaces of specimens annealed at 1125°C for 1h and fractured at room temperature during K testing. a.) a mixture of intergranular, cleavage, and a little dimple failure; b.) a cleavage fracture facet showing the cleavage crack initiates at a grain boundary and passes through the whole grain.

Fig. 5. Impact fracture energy vs. testing temperature. PNL and ORNL indicate the tests were performed at Pacific Northwest Laboratory and Oak Ridge National Laboratory, respectively.

Fig. 6. Fracture surfaces of specimens annealed at 1125°C for 1h and fractured at 100°C during J-integral testing. They are a mixture of dimple and intergranular (about 40%) failure. The arrows indicate typical intergranular feature.

Fig. 7. The dimpled fracture surface of a specimen annealed at 1125°C for 1h plus 890°C for 24h and fractured at RT during J-integral testing.

Fig. 8. The J-integral vs. crack growth curve generated from a specimen annealed at 1125°C for 1h plus 890°C for 24h during J-integral testing at RT. J_{IQ} is estimated as about 1100 kJ/m^2.

Fig. 9. the cleavage fracture surface of a specimen annealed at 1125°C for 1h plus 890°C for 24h and fractured at -50°C during K testing.

Fig. 10. Fracture toughness vs. testing temperature for specimens annealed either at 1125°C for 1h or at 1125°C for 1h plus 890°C for 24h.

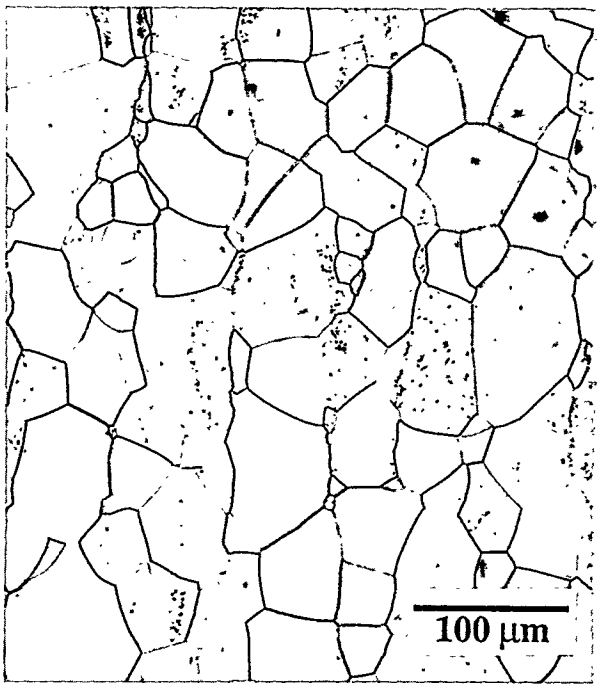

(a)

Fig. 1. Optical micrographs showing microstructure resulting from treatments of a) 1125°C/1 h/furnace cooled;

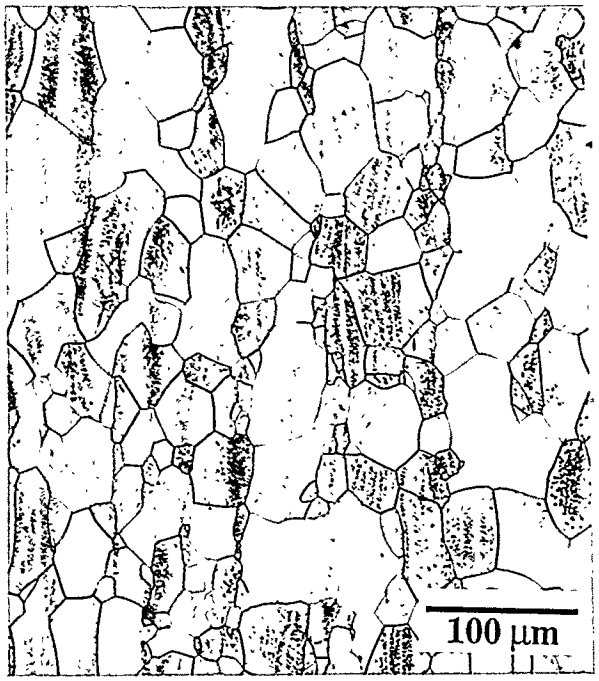

(b)

and b) 1125°C/1 h/furnace cooled plus 890°C/24h/furnace cooled.

(a)

Fig. 2. SEM micrographs showing the microstructure resulting from treatment of 1125°C1 h/furnace cooled plus 890°C/24 h/furnace cooled. a) secondary electron beam;

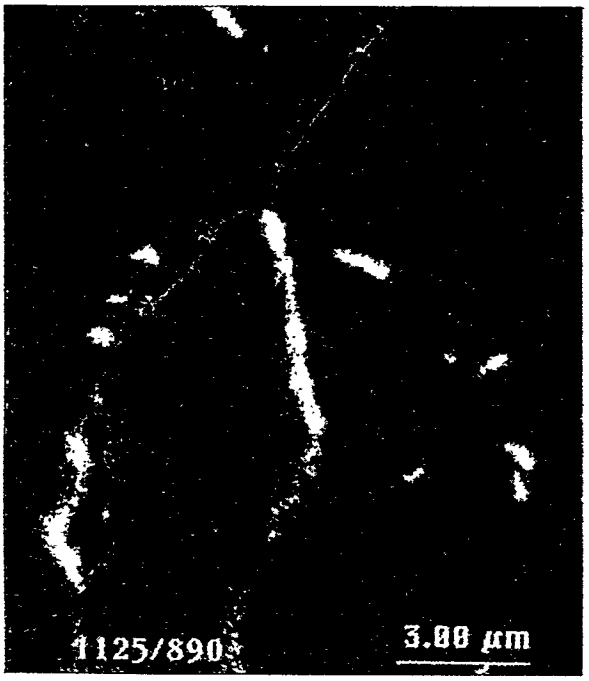

(b)

b) backscattered electron beam.

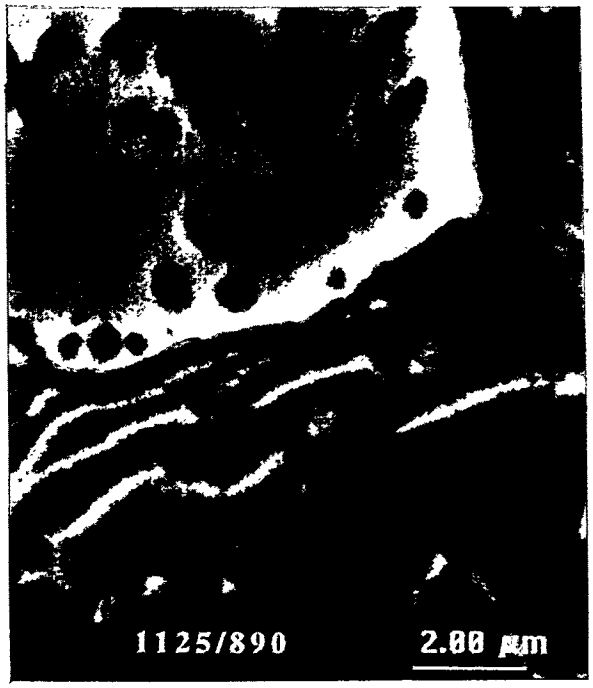

(a)

Fig. 3. SEM micrographs at higher mignification showing the microstructure resulting from treatment of 1125°C/1 h/furnace cooled plus 890°C/24 h/furnace cooled. a) pores and second phase;

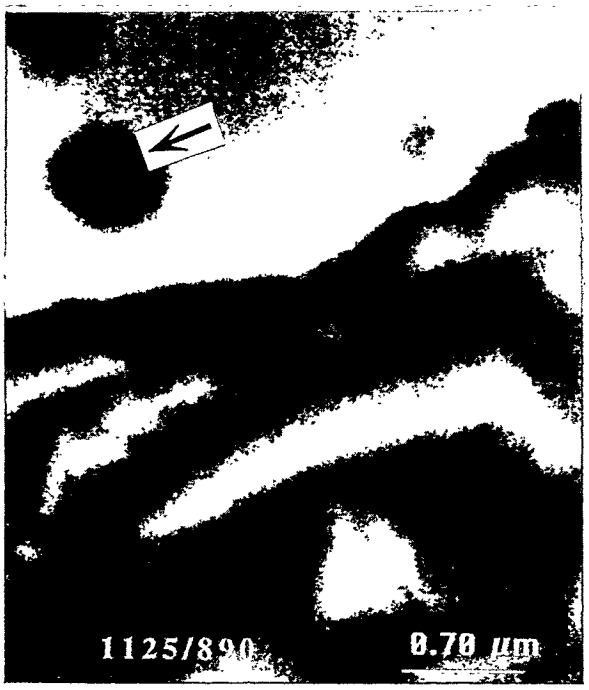

(b)

b) same location as (a) at higher magnification; the arrow indicates a precipitate particle.

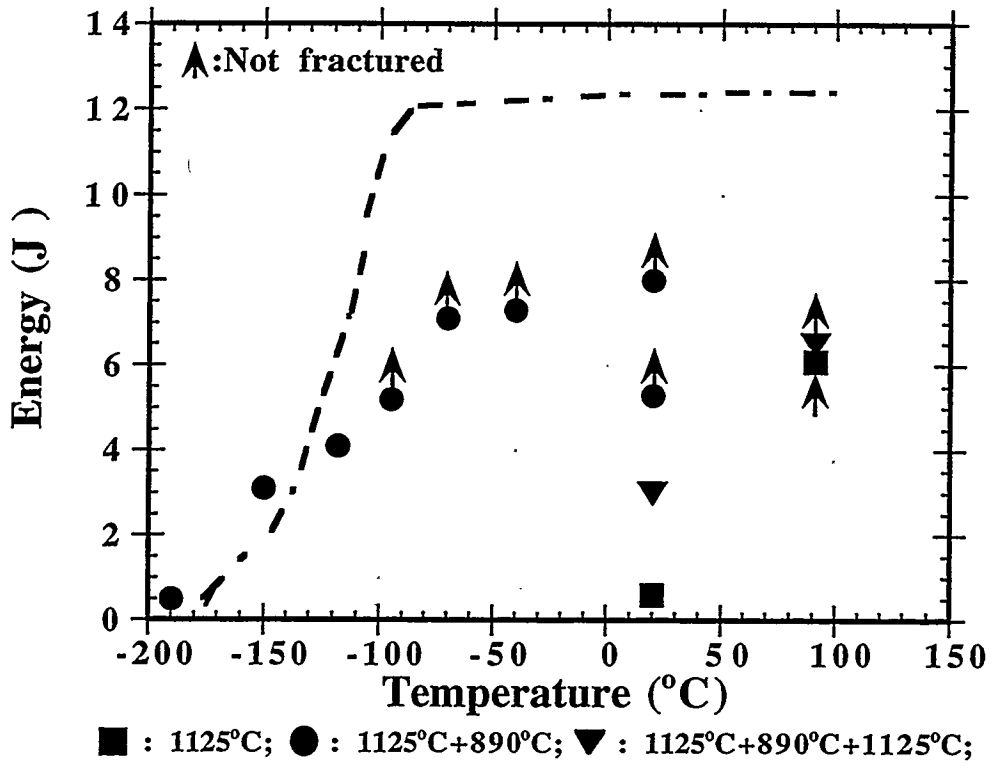

Fig. 4. Charpy V impact fracture energy vs. test temperature.

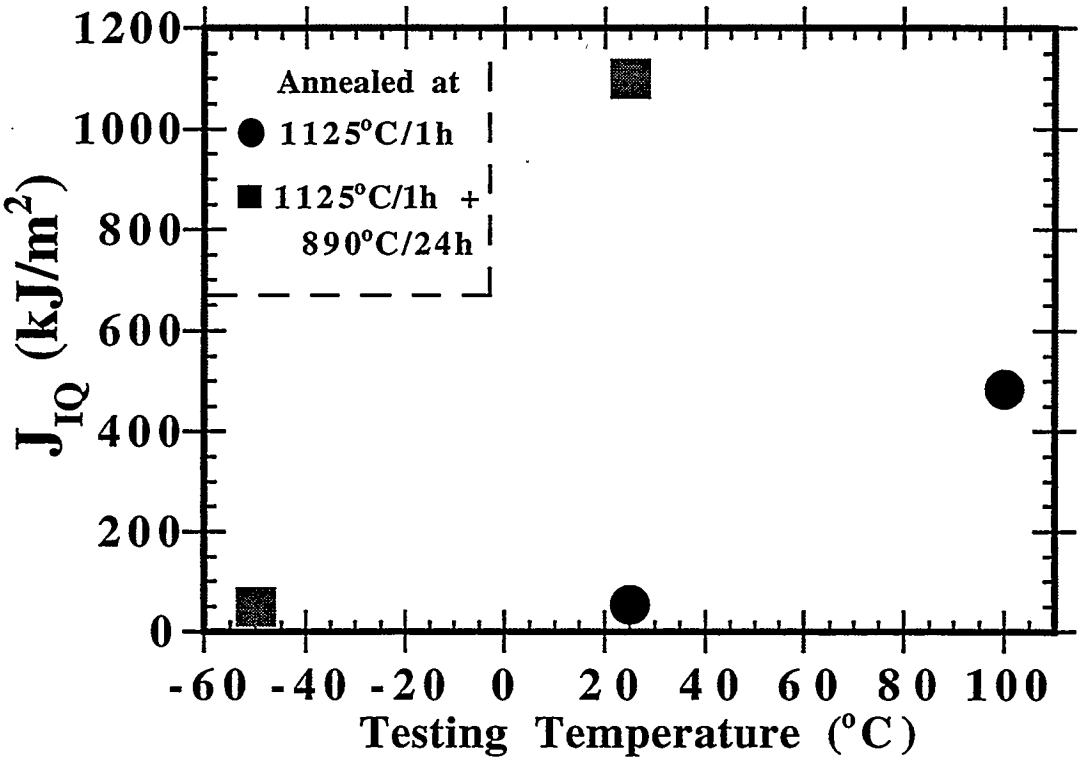

Fig. 5. Fracture toughness vs test temperature for specimens annealed either at 1125° for 1 h or at 1125°C for 1 h plus 890°C for 24 h.

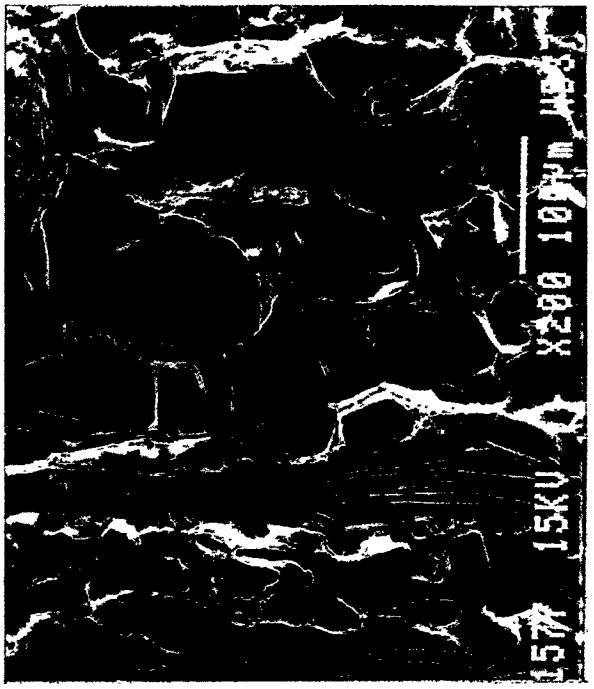

(a)

Fig. 6. Fracture surfaces of specimens annealed at 1125°C for 1 h and fractured at RT during K-testing. a) a mixture of intergranular, cleavage, and a little dimple failure;

(b)

b) a cleavage fracture facet showing that the cleavage crack initiates at a grain boundary and passes through the whole grain.

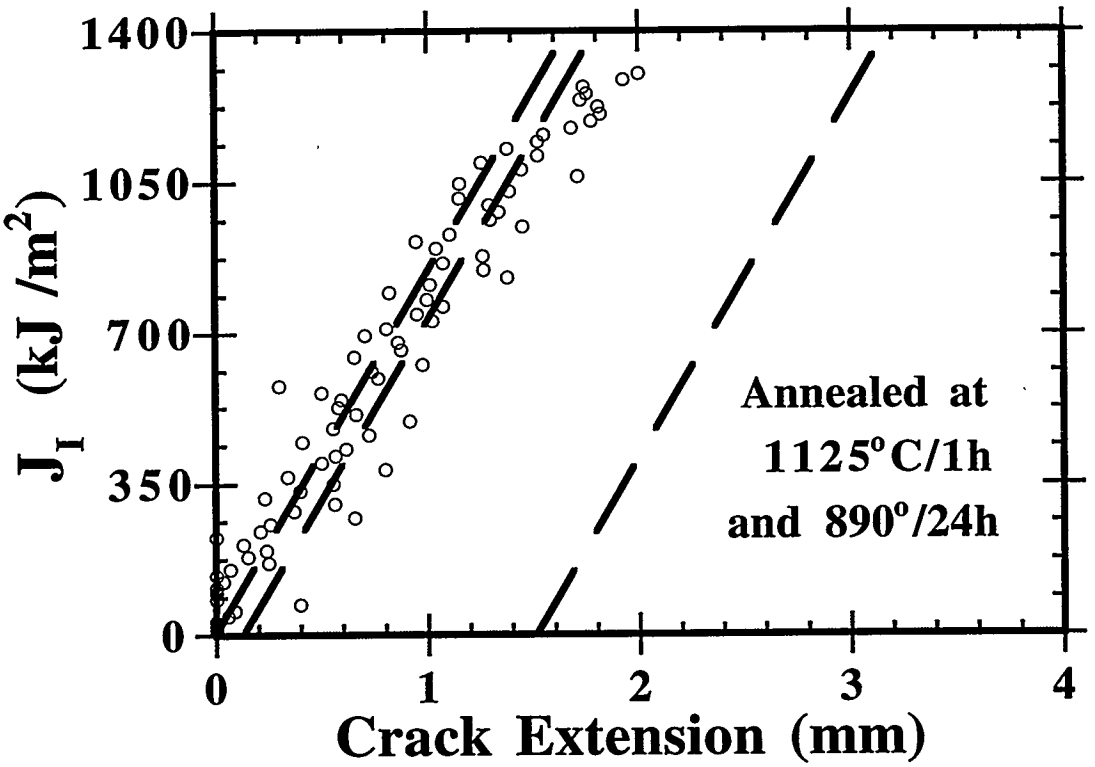

Fig. 7. The J-integral vs. crack growth curve generated from a specimen annealed at 1125°C for 1 h plus 890°C for 24 h during J-integral testing at RT. J_{IQ} is estimated at about 1100 kJ/m^2.

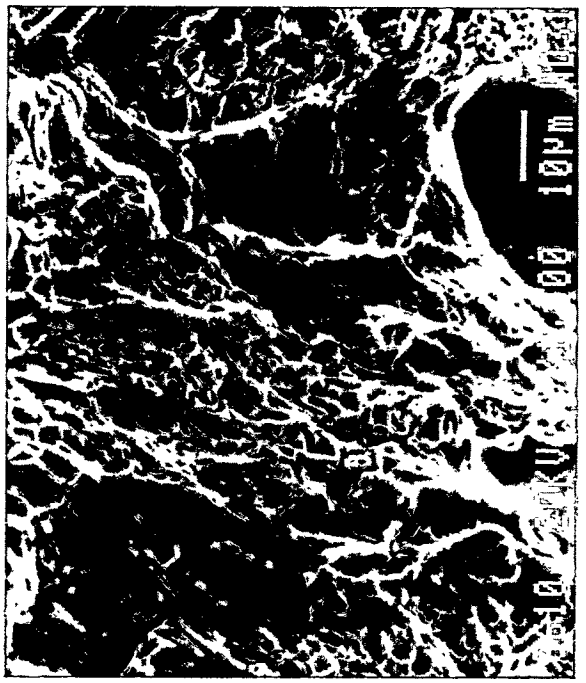

(a)

Fig. 8. The fracture surfaces of specimens annealed at 1125°C for 1 h plus 890°C for 24 h. a) dimpled fracture at RT during J-integral testing;

(b)

b) cleavage fracture -50°C during K testing.